



A systematic methodology to extend the applicability of a bioconversion model for the simulation of various co-digestion scenarios

Kovalovszki, Adam; Alvarado-Morales, Merlin; Fotidis, Ioannis; Angelidaki, Irini

Published in:
Bioresource Technology

Link to article, DOI:
[10.1016/j.biortech.2017.03.101](https://doi.org/10.1016/j.biortech.2017.03.101)

Publication date:
2017

Document Version
Peer reviewed version

[Link back to DTU Orbit](#)

Citation (APA):
Kovalovszki, A., Alvarado-Morales, M., Fotidis, I., & Angelidaki, I. (2017). A systematic methodology to extend the applicability of a bioconversion model for the simulation of various co-digestion scenarios. *Bioresource Technology*, 235, 157-166. <https://doi.org/10.1016/j.biortech.2017.03.101>

General rights

Copyright and moral rights for the publications made accessible in the public portal are retained by the authors and/or other copyright owners and it is a condition of accessing publications that users recognise and abide by the legal requirements associated with these rights.

- Users may download and print one copy of any publication from the public portal for the purpose of private study or research.
- You may not further distribute the material or use it for any profit-making activity or commercial gain
- You may freely distribute the URL identifying the publication in the public portal

If you believe that this document breaches copyright please contact us providing details, and we will remove access to the work immediately and investigate your claim.

1 **A systematic methodology to extend the applicability of a**
2 **bioconversion model for the simulation of various co-digestion**
3 **scenarios**

4

5 Adam Kovalovszki, Merlin Alvarado-Morales, Ioannis A. Fotidis, Irimi
6 Angelidaki*

7

8 Department of Environmental Engineering, Technical University of Denmark,
9 Bygningstorvet Bygning 115, DK-2800 Kgs. Lyngby, Denmark

10

11 *Corresponding Author: Department of Environmental Engineering, Technical
12 University of Denmark, DK-2800 Kgs. Lyngby, Denmark, Phone: (+45) 45251418;
13 Fax: (+45) 45933850; e-mail: iria@env.dtu.dk

14

15 **Running title**

16 Model simulating manure- and wastewater- based anaerobic co-digestion.

17

18 **ABSTRACT**

19 Detailed simulation of anaerobic digestion (AD) requires complex mathematical models
20 and the optimization of numerous model parameters. By performing a systematic
21 methodology and identifying parameters with the highest impact on process variables in
22 a well-established AD model, its applicability was extended to various co-digestion
23 scenarios. More specifically, the application of the step-by-step methodology led to the
24 estimation of a general and reduced set of parameters, for the simulation of scenarios
25 where either manure or wastewater were co-digested with different organic substrates.
26 Validation of the general parameter set involved the simulation of laboratory-scale data
27 from three continuous co-digestion experiments, treating mixtures of different organic
28 residues either at thermophilic or mesophilic conditions. Evaluation of the results
29 showed that simulations using the general parameter set fitted experimental data quite
30 well, indicating that it offers a reliable reference point for future simulations of
31 anaerobic co-digestion scenarios.

32 **KEYWORDS**

33 Anaerobic digestion, mathematical modeling, dynamic simulation, organic residue,
34 parameter set.

35 **1 Introduction**

36 Throughout the years, various mathematical models simulating both anaerobic
37 mono- and co-digestion processes have been proposed. From simpler empirical models
38 (Andrews, 1969; Graef and Andrews, 1974; Hill and Barth, 1977; Kleinstreuer and
39 Poweigha, 1982), to more complex ones (Angelidaki et al., 1999, 1993; Batstone et al.,

40 2002b; Costello et al., 1991; Siegrist et al., 1993). All of these models have been used to
41 describe, to a certain extent, the anaerobic digestion of complex substrates.

42 The majority of the complex models are specialized in anaerobic digestion of
43 specific feedstocks such as agricultural energy crops, residues, manures and wastewater
44 sludge. For instance, the Anaerobic Digestion Model No. 1 or ADM1 (Batstone et al.,
45 2002b) has been the most prominent among scientists working in the field of anaerobic
46 wastewater treatment processes and more recently in solid waste bioconversion
47 technologies. Likewise, the model (BioModel) proposed by Angelidaki et al. (1999)
48 gives a good description of manure-based anaerobic digestion systems. The BioModel
49 focuses on ammonia inhibition, which is often relevant in manure-based digestions, and
50 includes a detailed description of pH and temperature, in order to simulate free
51 ammonia concentrations. Compared to the ADM1, which expresses the concentration of
52 solid substrate and product components using the indirect Chemical Oxygen Demand
53 (COD), the BioModel features a more convenient, mass-based unit system. This allows
54 for the characterization of substrates and products using simpler sampling and
55 measurement techniques more appropriate for slurries and solid wastes, than COD.
56 Despite their extensive application, the optimal use of such complex models requires the
57 adjustment or modification of numerous parameters, depending on the type and nature
58 of the simulated case (Donoso-Bravo et al., 2011). General experience shows, however,
59 that the more parameters are contained in a mathematical model, the more difficult it
60 becomes to verify their values for individual cases. Specifically, the large number of
61 reactions and chemical species involved in these models gives a better description of the
62 process, but complicates modeling, and – depending on the system to be “modeled” –
63 the selection of the model itself to use. This also implies that existing complex models

64 are currently incapable of simulating dynamic processes describing diverse
65 experimental conditions, without a considerable amount of customization. Criteria to
66 select among models must weigh the trade-off between increased information
67 requirements and potentially better process description. Moreover, the model refinement
68 is an iterative procedure where the experimental and expert guided process of adding,
69 excluding, or modifying assumptions until a model that satisfactorily explains the
70 experimental data is obtained, is in general a difficult and time-consuming task (Sales-
71 Cruz and Gani, 2006).

72 Based on aforementioned premises, the objective of this study was to identify a set
73 of “benchmark” parameters that can be used without previous calibration for specific
74 digestion cases and which can satisfactorily describe different digestion cases such as
75 manure- or wastewater-based digestions. This was achieved through the application of a
76 systematic methodology, which essentially consisted of the following. First, parameter
77 selection was performed to reduce the parameter space for further treatment, based on a
78 detailed assessment of complex bioconversion model parameters, found to be reported
79 in literature with the greatest variations in their values. Second, detailed parameter
80 sensitivity analysis using Latin Hypercube Sampling (LHS) and the Partial Rank
81 Correlation Coefficient (PRCC) methods was performed, so that the less sensitive
82 parameters could be further discriminated/eliminated. Third, numerical optimization
83 using the Simulated Annealing (SA) method was carried out to estimate optimal
84 parameter values and statistical information was obtained to determine the feasibility of
85 the model parameters. Finally, the resulting set of optimized parameters was validated
86 with three selected experimental case studies, in order to demonstrate improved model
87 efficiency when using optimized parameters for simulation.

88 **2 Materials and Methods** Model Description

89 The core dynamic model (BioModel) of this work was developed by Angelidaki et
90 al. (1999, 1993) and describes the degradation of complex substrates, along with the co-
91 digestion of different types of organic wastes. In the BioModel, the substrate is
92 described in terms of its basic organic components' composition – carbohydrates, lipids
93 and proteins –, the concentration of intermediates such as volatile fatty acids (VFA) and
94 long-chain fatty acids (LCFA), and important inorganic components, such as ammonia,
95 phosphate, cations and anions. The model was upgraded to include the hydrolysis of
96 lipids so that it includes three enzymatic hydrolytic and eight bacterial steps, and
97 involves 19 chemical compounds, together with a detailed description of pH and
98 temperature characteristics. Free ammonia, VFA and LCFA constitute the primary
99 modulating factors. The BioModel was previously calibrated with experimental co-
100 digestion scenarios utilizing substrates rich in carbohydrates, proteins and lipids
101 (Angelidaki et al., 1999, 1997). For a detailed description of the model, see Table SI in
102 the Supplementary material.

103 **2.2 Computational Methods**

104 Initially written in Microsoft Pascal, and later translated to the Delphi Pascal
105 programming language, the BioModel was recently implemented in MATLAB,
106 combined with a Microsoft Excel-based data input and output platform. The MATLAB
107 model is able to simulate the AD process in one anaerobic fermenter, considering the
108 composition of the inoculum, a primary substrate and up to three optional co-substrates.
109 Organization and processing of parameters defining substrates, pump and flow rates,
110 metabolic steps and chemical components, as well as the collection of model output
111 variables was set up similar to as described by Angelidaki et al. (1999). Integration of

112 model equations in time and the selection of a suitable time step for calculations also
113 resembled the method outlined in this earlier publication, and for the solution of the
114 model ordinary differential equation system, MATLAB's *ode15s* solver was used.

115 **2.3 Systematic methodology**

116 The four steps describing the systematic methodology are depicted in Figure 1 and
117 are described further in the following subsections. During the analysis, the model
118 structure was kept as taken from the literature (Angelidaki et al., 1999).

119 **2.3.1 Step 1: Parameter selection**

120 In this step, a preliminary selection of the model parameters was performed based
121 on the assessment of available literature (Batstone et al., 2002a; Biernacki et al., 2013;
122 Bułkowska et al., 2015; López and Borzacconi, 2010; Lübken et al., 2007; Nguyen,
123 2014; Ramirez et al., 2009; Rivera-Salvador et al., 2014; Rosén and Jeppsson, 2006).
124 Details of this process are explained in the Supplementary material and the complete list
125 of parameters considered is shown in the Supplementary material, Table SII. As a
126 systematic reduction of the complete model parameter space and based on the
127 comparison of studies, biochemical parameters that showed significant variance and are
128 included in the BioModel were selected for subsequent sensitivity analysis in Step 2.

129 **2.3.2 Step 2: Parameter sensitivity analysis**

130 Following the parameter selection (Step 1), a detailed sensitivity analysis was
131 performed on the selected parameters, in order to evaluate the magnitude of the
132 parameters' individual effect on specific simulation output variables. The output
133 variables chosen were biogas and methane production, VFA and total ammonium
134 nitrogen-TAN concentration, pH, commonly reported as good indicators of the AD
135 process performance (Boe et al., 2010; Labatut and Gooch, 2012). Values of the

136 parameters selected in Step 1 were allowed to vary between lower and upper
137 boundaries, defined based on the literature assessment of Step 1, and sampling of the
138 available parameter space was performed with the Latin Hypercube Sampling (LHS)
139 method (McKay, 1992; McKay et al., 1979). LHS was an integral part of the analysis,
140 in order to make sure that the parameter values were selected from the whole range
141 available, avoiding bias and maintaining statistical accuracy. Concerning the
142 distribution of parameter intervals by the LHS method, uniform parameter distribution
143 was assumed (Manache and Melching, 2007), and the number of parameter sample sets
144 generated by the method was ten times the number of parameters selected for analysis.

145 Following the sampling process, simulations were performed with every set of
146 parameter samples generated previously. The length of the simulated periods
147 corresponded to the periods where experimental data were available. Furthermore, to
148 reduce computational demand, four approximately equidistant time points of each case
149 simulation period were selected and only the output variable values of these time points
150 were used thereafter.

151 Sampling-based Partial Rank Correlation Coefficient (PRCC) method (Marino et
152 al., 2008; Pennington, 2015; Wu et al., 2013; Zi, 2011) was used to perform sensitivity
153 analysis. As the PRCC method does not account for time as an independent variable,
154 PRCC analyses for the previously selected, equidistant time points were conducted
155 separately, in order to produce statistically representative results for complete
156 simulation periods. Further to that, for PRCC results to be considered relevant, their
157 probability values (p-values) were required to be smaller than 0.05 (Jackson and
158 Radunskaya, 2015). For each case study, results of the PRCC analyses for individual
159 time points were combined, providing an aggregate PRCC value over the entire

160 simulated period. Parameters were ranked according to their PRCC values to define the
161 most sensitive parameters with respect to each model output variable specified in Step
162 2. Both LHS and the PRCC analyses were carried out using the MATLAB-based
163 Sampling and Sensitivity Analyses Tool (SaSAT) (Hoare et al., 2008).

164 **2.3.3 Step 3: Parameter estimation**

165 After identification of the most sensitive parameters in Step 2, numerical estimation
166 of their values was performed for both case studies. Variation in parameter values was
167 allowed according to lower and upper parameter boundaries specified in Step 2. The
168 parameters were estimated by minimization of the sum of squares of the differences
169 between predicted and experimental data sets (see Table SIII of the Supplementary
170 material). For the optimization task, the Simulated Annealing (SA) method was used
171 (Ingber, 1996; Kirkpatrick et al., 1983). Implementation of the method was done in
172 MATLAB, using the *simulannealbnd* function. Each case study was simulated with 250
173 iterations (a number used also by López and Borzacconi (2010)), in three consecutive
174 parameter estimation cycles to support the results of the stochastic optimization method
175 statistically. At the last step, SA iteration histories, objective function values and
176 estimated parameter values were collected from all simulations, and were used for
177 comparing the different scenarios on a quantitative and qualitative basis.

178 **2.3.4 Step 4: Validation and evaluation of the results**

179 First, performance criteria simulations – benchmark simulations – with the original
180 model parameter values were compared against simulations using the optimized
181 parameter values identified in Step 3, for both case studies used during parameter
182 estimation. Second, following the unification of optimized parameter values used in
183 case study 1 and 2 – by calculating the mathematical average of the respective

184 parameter values – validation of optimized parameters was performed with the data of
185 three lab-scale CSTR experiments. Finally, conclusions were drawn based on the results
186 of validation.

187 **2.4 Case studies**

188 Below a short overview of the two experimental case studies, which were used
189 during parameter estimation is provided. For further details on simulated substrate and
190 process characteristics, see the Supplementary material, Table SIV and SV.

191 **2.4.1 Case study 1 (C1)**

192 Process data was collected from the doctoral dissertation of Schön (2009). In his
193 work, the author investigated the applicability of ADM1 for the simulation of the AD
194 process of a demonstration biogas plant, and lab-scale reactors fed only with manure.
195 The reactor selected for simulation had a volume of 75 L and was operated at
196 mesophilic conditions (37 °C), with a hydraulic retention time (HRT) of 10 days, in four
197 consecutive periods. Period 1 (day 0-8): no influent feed, operated as batch with only
198 inoculum. Period 2 (day 9-15), Period 3 (day 16-22) and Period 4 (day 23-30) fed solely
199 with manure of varying composition (Supplementary material, Table SIV). Due to the
200 simplicity of the experimental setup and the availability of relevant data such as input
201 manure characteristics, biogas production and pH, this case was selected as the initial
202 case study for analysis.

203 **2.4.2 Case study 2 (C2)**

204 A continuous lab-scale experiment, carried out by Wang et al. (2016) using GTO
205 and ammonia as co-substrates, was used as the second case study. The reactor had a
206 working volume of 1.8 L, its inoculum originated from digestion of a mixture of cattle
207 and pig manure, while cattle manure served as the primary substrate for reactor feeding

208 (Supplementary material, Table SV). Reactor temperature was kept at 54 °C throughout
209 the whole experiment. Feeding took place with an HRT of 15 days, throughout the
210 experiment. The experiment was divided into two main phases; in the first phase,
211 manure feed was mixed with rapidly increasing concentrations of GTO, raising the
212 organic loading rate (OLR) from 3.2 g-VS L⁻¹d⁻¹ to 5 g-VS L⁻¹d⁻¹ in 54 days, which
213 ended with the collapse of the reactor. Following re-inoculation, the reactor in the
214 second phase was fed with manure and a gradually increasing concentration of GTO,
215 reaching from 3.2 to 4 g-VS L⁻¹d⁻¹ added organic material in 91 days, after which OLR
216 was kept stable. Meanwhile, ammonia addition in this last period increased from 2.1 to
217 5 g-N L⁻¹, during the course of 157 days. Thus for the simulation, 9 feeding periods
218 were defined, based on data provided by Wang et al. (not shown).

219 **3 Results and Discussion**

220 Base case simulations for the two case studies (C1 and C2) were generated with the
221 original BioModel parameters. The response of the model in terms of biogas or methane
222 productivities, and total VFA concentrations (where applicable) is shown in Figure 2a
223 (C1) and Figure 2b (C2), and are discussed in the following sections. pH simulations
224 were included in the Supplementary material (Figure S1 and S2).

225 Following the steps outlined in the systematic methodology, 44 parameters were
226 initially selected in Step 1 for sensitivity analysis, with lower and upper boundaries
227 defined based on the smallest and largest values reported for anaerobic digestion of
228 complex substrates. The list of initially selected parameters, along with their lower and
229 upper limits, can be found in the Supplementary material, Table SVI. In Step 2, the
230 most sensitive parameters were identified for the individual estimation case studies
231 (average PRCC values shown in Table SVII of the Supplementary material). Out of 44

232 initial parameters tested, model output variables were found to be sensitive to mainly 13
233 specific parameters. These 13 parameters included: $\text{Hydr}_{\text{carb,in}}$, $\text{Hydr}_{\text{prot,in}}$, K_{SAA} , K_{SHPr} ,
234 K_{SHVal} , K_{SHAc} , $\text{K}_{\text{iNH}_3,\text{HAc}}$, pK_{hAc} , K_{dAA} , K_{dHPr} , K_{dHBut} , K_{dHVal} and K_{dHAc} . These
235 parameters and their quantified effect (PRCC values) on the output variables are shown
236 in Figure 3. As seen from the graphs, parameter effects show significant variations
237 depending on the output variables considered, but the trends in PRCC values, and thus
238 the overall parameter effects on the simulated systems appear similar. Once the most
239 sensitive parameters were identified, Step 3 was then executed, the results of which are
240 discussed in the next sections, for each case study respectively.

241 **3.1 Case study 1 (C1)**

242 In the first benchmark simulation, the response of the model with the original set of
243 parameters is shown in red color in Figure 2a. As observed, model response fitted well
244 the trend exhibited by experimental data, particularly in Periods 1, 2 and 3 at which
245 biogas production increased – due to an increase in the organic loading rate – and then
246 stabilized at a new steady state level. In contrast with the trend exhibited by the
247 experimental data during Period 4, where biogas production is shown to decrease
248 throughout the whole period, the model predicted a slight decrease at the beginning and
249 subsequently reached a new steady state level. This discrepancy is explained by the fact
250 that during this operational period experimental values were not recorded properly as
251 pointed out by the authors. Figure 2a shows in green color the response of the model
252 when the set of optimized parameters (see Table II) was used. Although qualitative
253 improvement is difficult to assess, improvements in the fitting were obtained. This was
254 further confirmed by the value of the objective function, which was reduced from 0.498
255 to 0.356 representing a 28.5% improvement in the model response (Table I).

256 Meanwhile, the quality of the pH simulation was unchanged and remained highly
257 accurate (see Figure S1 in Supplementary material). Compared to the ADM1 simulation
258 that is shown in Figure 2a in blue color, both the benchmark and optimized simulations
259 fit experimental data with high accuracy, especially in Period 2, where a rapid increase
260 in biogas productivity is observed. This indicates that the BioModel appeared to
261 produce more accurate simulations for anaerobic manure digestion than the ADM1.

262 **3.2 Case study 2 (C2)**

263 In the second benchmark simulation, the response of the model with the original set of
264 parameters is shown in Figure 2b in red color. First, two operational periods can be
265 observed with a considerable degree of uncertainty. Operational Period 2 between days
266 50 and 80, where simulated methane productivity increased more rapidly compared to
267 the experimental trend, while the simulated total VFA concentrations only reached
268 about half of the experimental values. Periods 8 and 9 (between day 300 and 420), on
269 the other hand, showed an opposite trend, with a significant delay in the decrease of
270 methane productivity and an overestimation in total VFA concentration simulated. The
271 value of the objective function for the benchmark simulation was found to be 461.289
272 (see Table I). Figure 2b shows in green the response of the model when the set of
273 optimized parameters (see Table II) were used. As observed, by using the optimized
274 parameters a significant improvement (82.5%) was obtained in the objective function
275 value (see Table I), which is well represented by the satisfactory fit of the total VFA
276 experimental data – particularly between days 300 and 420 (see Figure 2b, bottom in
277 green).

278 **3.3 Parameter set validation**

279 As a result of the parameter optimization process carried out using the two
280 aforementioned case studies, a general set of estimated parameters was compiled (see
281 Table II), with parameter boundaries defined based on the lowest and highest optimized
282 parameter values used by the SA algorithm. For validating the above, generally
283 applicable set of parameters, three case studies are described below. They were selected
284 from a wide range of experiments, and covered manure co-digestion with
285 carbohydrates, manure co-digestion with complex substrates and wastewater co-
286 digestion with complex substrates.

287 **3.3.1 Validation case study 1 (V1)**

288 Experimental material for the first validation case scenario was taken from
289 Søndergaard et al. (2015), who investigated the effect of meadow grass on biogas
290 productivity, when added to manure and co-digested in CSTR-type reactors
291 (Supplementary material, Table SVIII). By gradually increasing the concentration of
292 meadow grass in the reactor, while using the same manure substrate, the experiment had
293 four distinct feeding periods. Period 1 (day 0-12): manure feed without additional
294 meadow grass. Period 2 (day 13-61): manure feed with 12 g L⁻¹ meadow grass. Period 3
295 (day 62-91): manure feed with 23 g L⁻¹ meadow grass. Period 4 (day 92-107): manure
296 feed with 34 g L⁻¹ meadow grass. Operation temperature was 54 °C and the working
297 volume was 3.5 L.

298 Benchmark simulations can be seen in Figure 4 in red, covering biogas productivity
299 (top) and total VFA concentrations (bottom). Although the trend in total VFA
300 concentrations is well captured by the BioModel, the total amounts are higher than the
301 experimentally measured values. This is inversely true for the biogas productivity

302 simulation, where the curve in the second half of Period 2 and in Period 3 and 4 falls
303 below the zone where experimental points are found. A clear improvement is achieved
304 in biogas productivity simulation using the general set of optimized parameters (curves
305 in green), as the curve becomes higher, fitting experimental data quite well in Period 2
306 and 3 and almost reaching experimental levels in Period 4. This is achieved by
307 increasing the simulated total VFA concentration slightly, which decreases simulation
308 accuracy somewhat further in Period 3 and 4. However, it also provides a better
309 description of the elevated total VFA concentration in the first half of Period 2 and
310 keeps the overall trend marked by experimental points.

311 **3.3.2 Validation case study 2 (V2)**

312 A complex experiment published by Fitamo et al. (2016a, 2016b) served as source
313 material for the second validation case study, where the authors were co-digesting
314 mixed wastewater sludge (MS) with different urban organic wastes (UOW), such as
315 food waste, grass clippings and garden waste (Supplementary material, Table SIX).
316 Although the experiment involved two reactors, only the first one was considered in
317 present study. According to the description of the process, five feeding periods were
318 defined during the experiment, where the first covered only MS digestion and UOW
319 were added from Period 2. Between Period 2 and 5, the volatile solid-based mixture of
320 the four substrates was kept constant, meaning an approximately 10:68:15:7 mixing
321 ratio for mixed sludge, food waste, grass clippings and garden waste, respectively. The
322 distribution of feeding periods is as follows. Period 1 (day 0-75): MS digestion with an
323 HRT of 30 days. Period 2 (day 76-130): MS and UOW, HRT of 30 days. Period 3 (day
324 131-164): MS and UOW, HRT of 20 days. Period 4 (day 165-203): MS and UOW,

325 HRT of 15 days. Period 5 (day 204-230): MS and UOW, HRT of 10 days. The reactor
326 working volume was 3 L and operation temperature was 55 °C.

327 Results of the simulation carried out by Fitamo et al., with default parameters
328 (Figure 5, curves in blue) indicate that biogas productivity (top) was captured very well,
329 along with total ammonia concentrations (bottom) outside Period 2. The total VFA
330 simulation (middle), however, showed higher levels than seen during the experiment.
331 By running simulations with the general set of optimized parameters (Figure 5, curves
332 in green), significant improvements were achieved in fitting experimental data.
333 Moreover, the simulation of total ammonia concentrations was now highly accurate,
334 including that of Period 2, while the biogas productivity did not change considerably.
335 Interestingly, simulated total VFA concentrations were lowered, to about half of what
336 was simulated by Fitamo et al., providing a more accurate fit of experimental data. The
337 simulated peak in Period 2 is most probably the result of starting the addition of UOW,
338 where food waste contained high amounts of soluble lipids and carbohydrates. In
339 contrast, low experimental values might indicate a microorganic community already
340 well adapted to such concentrations.

341 **3.3.3 Validation case study 3 (V3)**

342 For the simulation of the third validation case study, lipid hydrolysis with first-order
343 kinetics was included as a structural part of the BioModel and it was set up assuming
344 inert and soluble fractions as described in Miron et al. (2000). Information about
345 substrates and process decisions used during the case study were collected from Fezzani
346 and Cheikh (2008, 2007), who described the co-digestion of olive mill wastewater and
347 olive mill solid waste at different HRTs and influent concentrations (Supplementary
348 material, Table SX). The selected experiment used an influent total Chemical Oxygen

349 Demand (TCOD) of 80 g-COD L^{-1} and was divided into three periods. Period 1 (day 0-
350 70): mixed feed with an HRT of 36 days. Period 2 (day 71-120): mixed feed with an
351 HRT of 24 days. Period 3 (day 121-150): mixed feed with an HRT of 12 days. The
352 reactor, despite being a tubular type, was completely mixed and had a working volume
353 of 18 L. Operation temperature was $37 \text{ }^{\circ}\text{C}$.

354 The response of the model with the original set of parameters is shown in Figure 6
355 in red. For operation Period 1 and 2, qualitatively the model prediction was good.
356 However, the model was not able to forecast the third period at which a rapid decrease
357 in biogas productivity and accumulation of VFA were observed. Another important
358 aspect to point out is the sharp maximum in biogas productivity that the model predicts
359 in Period 1 (between days 1-5), which happens early, yet is well in line with the
360 experimental trend. Using the general set of optimized parameters and together with a
361 slight increase in biogas productivity in Period 1 and 2 (Figure 6, top), a favorable
362 increase in total VFA concentrations was experienced, visible principally in Period 3
363 (Figure 6, bottom).

364 When compared to the performance of ADM1 as seen in Figure 6, the BioModel
365 performed better for the simulation of the initial increase in biogas production, however,
366 it was not able to simulate the rapid decline in biogas productivity (Figure 6, top) and
367 the proportional increase in total VFA concentrations (Figure 6, bottom) seen in the last
368 feeding period. This is most likely because the BioModel does not include a VFA
369 inhibition term effective on the growth of methanogenic microorganic groups, while
370 these inhibitory kinetics were added to the ADM1 by Fezzani and Cheikh. Another way
371 to decrease biogas productivity forecasted by the BioModel would have been the
372 reduction of the ammonia inhibition term K_{i,NH_3} (whose value was 0.259 before and

373 became 0.275 after optimization), which takes effect on acetoclastic methanogens.
374 Being the overall most sensitive parameter among the 13 parameters identified in Step 2
375 of the methodology, this would have improved the fit in Period 3. Nevertheless, this
376 adjustment would not be feasible, as the authors have stated that ammonia concentration
377 was kept constant, at a low concentration of around 1.3 g-N L^{-1} , throughout the whole
378 experiment (Fezzani and Cheikh, 2008). Assuming, however, that the rapid decline in
379 biogas productivity was due to the inhibition of acetoclastic methanogenic groups by
380 the accumulation of phenolic compounds (Borja et al., 1997) justifies the performance
381 of the BioModel, as this factor is not accounted for in the model and thus could not
382 decrease the productivity in Period 3.

383 **3.4 Evaluation**

384 The evaluation of above three validation case studies showed that by restricting
385 future parameter estimations to the 13 sensitive parameters shown, significant
386 improvements can be expected in simulation results. Further to the above, results of the
387 present study indicate that in order to improve BioModel simulations, especially for
388 wastewater-based co-digestion, process inhibition dynamics should be redesigned,
389 considering certain effects that are currently missing in the microorganic growth
390 equations. This will form part of subsequent studies carried out by the authors.

391 As a general comment and regarding the data accuracy of the three case studies,
392 findings of present study and earlier work of Zielesny (2016) indicate that the inclusion
393 of experimental measurement errors in objective function calculations might be
394 favorable. Using such information, weighing the importance of experimental data points
395 would become possible, in order to discount for the effect of outliers and improve the
396 optimization system to be solved.

397 **4 Conclusions**

398 The aim of present work was to develop a parameter estimation methodology, for
399 the improvement of anaerobic digestion modelling. By identifying the sensitive
400 parameters of a complex bioconversion model (BioModel) and estimating their optimal
401 values, it was found that the model was able to simulate the most relevant process
402 variables with improved accuracy. Although the microbial growth expressions in the
403 BioModel need further improvement for accurately describing certain inhibition
404 phenomena, using the optimized parameter set was proven to expand its applicability
405 for simulating both manure- and wastewater-based co-digestion cases, at either
406 mesophilic or thermophilic conditions.

407 **Acknowledgements**

408 The authors would like to thank Lars Ellegaard for providing valuable feedback on
409 present work. The project was supported by Energinet.dk, through the project ForskEL-
410 12197 titled “Improving synergy and robustness of manure co-digestion process”.

411 **Conflict of Interest**

412 The authors claim no conflict of interest concerning any part of the work presented
413 here.

414 **References**

- 415 1. Andrews, J.F., 1969. Dynamic model of the anaerobic digestion process. *J. Sanit.*
416 *Eng. Div.* 95, 95–116.
- 417 2. Angelidaki, I., Ellegaard, L., Ahring, B.K., 1999. A comprehensive model of
418 anaerobic bioconversion of complex substrates to biogas. *Biotechnol. Bioeng.* 63, 363–
419 372.
- 420 3. Angelidaki, I., Ellegaard, L., Ahring, B.K., 1997. Modelling Anaerobic Codigestion
421 of Manure with Olive Oil Mill Effluent. *Water Sci. Technol.* 36, 263–270.
- 422 4. Angelidaki, I., Ellegaard, L., Ahring, B.K., 1993. A mathematical model for
423 dynamic simulation of anaerobic digestion of complex substrates: Focusing on
424 ammonia inhibition. *Biotechnol. Bioeng.* 42, 159–166.
- 425 5. Batstone, D.J., Keller, J., Angelidaki, I., Kalyuzhny, S. V., Pavlostathis, S.G., Rozzi,
426 A., Sanders, W.T.M., Siegrist, H., Vavilin, V.A., 2002. Anaerobic digestion model no. 1
427 (ADM1). IWA Publishing, London.
- 428 6. Batstone, D.J., Keller, J., Angelidaki, I., Kalyuzhnyi, S. V., Pavlostathis, S.G.,
429 Rozzi, A., Sanders, W.T., Siegrist, H., Vavilin, V. a., 2002. The IWA Anaerobic
430 Digestion Model No 1 (ADM1). *Water Sci. Technol.* 45, 65–73.
- 431 7. Biernacki, P., Steinigeweg, S., Borchert, A., Uhlenhut, F., 2013. Application of
432 Anaerobic Digestion Model No. 1 for describing anaerobic digestion of grass, maize,
433 green weed silage, and industrial glycerine. *Bioresour. Technol.* 127, 188–194.
- 434 8. Boe, K., Batstone, D.J., Steyer, J.-P., Angelidaki, I., 2010. State indicators for
435 monitoring the anaerobic digestion process. *Water Res.* 44, 5973–5980.

- 436 9. Borja, R., Alba, J., Banks, C.J., 1997. Impact of the main phenolic compounds of
437 olive mill wastewater (OMW) on the kinetics of acetoclastic methanogenesis. *Process*
438 *Biochem.* 32, 121–133.
- 439 10. Bułkowska, K., Białobrzewski, I., Gusiatin, Z.M., Klimiuk, E., Pokój, T., 2015.
440 ADM1-based modeling of anaerobic codigestion of maize silage and cattle manure –
441 calibration of parameters and model verification (part II). *Arch. Environ. Prot.* 41, 20–
442 27.
- 443 11. Costello, D.J., Greenfield, P.F., Lee, P.L., 1991. Dynamic modelling of a single-
444 stage high-rate anaerobic reactor-I. Model derivation. *Water Res.* 25, 847–858.
- 445 12. Donoso-Bravo, A., Mailier, J., Martin, C., Rodríguez, J., Aceves-Lara, C.A.,
446 Wouwer, A. Vande, 2011. Model selection, identification and validation in anaerobic
447 digestion: A review. *Water Res.* 45, 5347–5364.
- 448 13. Fezzani, B., Cheikh, R.B., 2008. Modelling of the mesophilic anaerobic co-
449 digestion of olive mill wastewater with olive mill solid waste using anaerobic digestion
450 model No. 1 (ADM1). *Bioresour. Technol.* 99, 6565–6577.
- 451 14. Fezzani, B., Cheikh, R.B., 2007. Anaerobic co-digestion of olive mill wastewater
452 with olive mill solid waste in a tubular digester at mesophilic temperature. *Bioresour.*
453 *Technol.* 98, 769–774.
- 454 15. Fitamo, T., Boldrin, A., Boe, K., Angelidaki, I., Scheutz, C., 2016a. Co-digestion of
455 food and garden waste with mixed sludge from wastewater treatment in continuously
456 stirred tank reactors. *Bioresour. Technol.* 206, 245–254.
- 457 16. Fitamo, T., Boldrin, A., Dorini, G., Boe, K., Angelidaki, I., Scheutz, C., 2016b.
458 Optimising the anaerobic co-digestion of urban organic waste using dynamic
459 bioconversion mathematical modelling. *Water Res.* 106, 283–294.

- 460 17. Graef, S.P., Andrews, J.F., 1974. Mathematical modeling and control of anaerobic
461 digestion. *Water Res.* 8, 261–289.
- 462 18. Hill, D.T., Barth, C.L., 1977. A dynamic model for simulation of animal waste
463 digestion. *J. Water Pollut. Control Fed.* 49, 2129–2143.
- 464 19. Hoare, A., Regan, D.G., Wilson, D.P., 2008. Sampling and sensitivity analyses tools
465 (SaSAT) for computational modelling. *Theor. Biol. Med. Model.* 5, 4.
- 466 20. Ingber, L., 1996. Adaptive simulated annealing (ASA): Lessons learned. *Control*
467 *Cybern.* 25, 33–54.
- 468 21. Jackson, T., Radunskaya, A., 2015. *Applications of Dynamical Systems in Biology*
469 *and Medicine.* Springer-Verlag, New York.
- 470 22. Kirkpatrick, S., Gelatt, C. D., Vecchi, M. P., 1983. Optimization by Simulated
471 Annealing. *Science* (80-). 220, 671–680.
- 472 23. Kleinstreuer, C., Poweigha, T., 1982. Dynamic simulator for anaerobic digestion
473 processes. *Biotechnol. Bioeng.* 24, 1941–1951.
- 474 24. Labatut, R. a., Gooch, C. a., 2012. Monitoring of Anaerobic Digestion Process to
475 Optimize Performance and Prevent System Failure, in: *Proceedings of Got Manure?*
476 *Enhancing Environmental and Economic Sustainability.* pp. 209–225.
- 477 25. López, I., Borzacconi, L., 2010. Modelling of slaughterhouse solid waste anaerobic
478 digestion: Determination of parameters and continuous reactor simulation. *Waste*
479 *Manag.* 30, 1813–1821.
- 480 26. Lübken, M., Wichern, M., Schlattmann, M., Gronauer, A., Horn, H., 2007.
481 Modelling the energy balance of an anaerobic digester fed with cattle manure and
482 renewable energy crops. *Water Res.* 41, 4085–4096.

- 483 27. Manache, G., Melching, C.S., 2007. Sensitivity of Latin Hypercube Sampling To
484 Sample Size and Distributional Assumptions, in: Proceedings of the 32nd Congress of
485 the IAHR. pp. 1–10.
- 486 28. Marino, S., Hogue, I.B., Ray, C.J., Kirschner, D.E., 2008. A Methodology for
487 Performing Global Uncertainty and Sensitivity Analysis in Systems Biology. *J. Theor.*
488 *Biol.* 254, 178–196.
- 489 29. McKay, M.D., 1992. Latin hypercube sampling as a tool in uncertainty analysis of
490 computer models, in: Proceedings of the 1992 Winter Simulation Conference. pp. 557–
491 564.
- 492 30. McKay, M.D., Beckman, R.J., Conover, W.J., 1979. A Comparison of Three
493 Methods for Selecting Values of Input Variables in the Analysis of Output from a
494 Computer Code. *Technometrics* 42, 55–61.
- 495 31. Miron, Y., Zeeman, G., Van Lier, J.B., Lettinga, G., 2000. The role of sludge
496 retention time in the hydrolysis and acidification of lipids, carbohydrates and proteins
497 during digestion of primary sludge in CSTR systems. *Water Res.* 34, 1705–1713.
- 498 32. Nguyen, H.H., 2014. Modelling of food waste digestion using ADM1 integrated
499 with Aspen Plus. University of Southampton.
- 500 33. Pennington, H.M., 2015. Applications of Latin Hypercube Sampling Scheme and
501 Partial Rank Correlation Coefficient Analysis to Mathematical Models on Wound
502 Healing. Western Kentucky University.
- 503 34. Ramirez, I., Mottet, A., Carrère, H., Déléris, S., Vedrenne, F., Steyer, J.P., 2009.
504 Modified ADM1 disintegration/hydrolysis structures for modeling batch thermophilic
505 anaerobic digestion of thermally pretreated waste activated sludge. *Water Res.* 43,
506 3479–3492.

507 35. Rivera-Salvador, V., López-Cruz, I.L., Espinosa-Solares, T., Aranda-Barradas, J.S.,
508 Huber, D.H., Sharma, D., Toledo, J.U., 2014. Application of Anaerobic Digestion
509 Model No. 1 to describe the syntrophic acetate oxidation of poultry litter in
510 thermophilic anaerobic digestion. *Bioresour. Technol.* 167, 495–502.

511 36. Rosén, C., Jeppsson, U., 2006. Aspects on ADM1 Implementation within the BSM2
512 Framework, Technical report. Lund.

513 37. Sales-Cruz, M., Gani, R., 2006. Model discrimination and parameter estimation
514 through sensitivity analysis. *Comput. Aided Chem. Eng.* 21, 625–631.

515 38. Schön, M., 2009. Numerical Modelling of Anaerobic Digestion Processes in
516 Agricultural Biogas Plants. University of Innsbruck.

517 39. Siegrist, H., Renggli, D., Gujer, W., 1993. Mathematical modelling of anaerobic
518 mesophilic sewage sludge treatment. *Water Sci. Technol.* 27, 25–36.

519 40. Sørensgaard, M.M., Fotidis, I.A., Kovalovszki, A., Angelidaki, I., 2015. Anaerobic
520 Co-digestion of Agricultural Byproducts with Manure for Enhanced Biogas Production.
521 *Energy and Fuels* 29, 8088–8094.

522 41. Wang, H., Fotidis, I.A., Angelidaki, I., 2016. Ammonia-LCFA synergetic co-
523 inhibition effect in manure-based continuous biomethanation process. *Bioresour.*
524 *Technol.* 209, 282–289.

525 42. Wu, J., Dhingra, R., Gambhir, M., Remais, J. V, 2013. Sensitivity analysis of
526 infectious disease models: methods, advances and their application. *J. R. Soc. Interface*
527 10, 20121018.

528 43. Zi, Z., 2011. Sensitivity analysis approaches applied to systems biology models. *IET*
529 *Syst. Biol.* 5, 336–346.

530 44. Zielesny, A., 2016. From curve fitting to machine learning : an illustrative guide to
531 scientific data analysis and computational intelligence, second. ed. Springer
532 International Publishing, Switzerland.

533 **Tables**

534 **Table I.** A comparison of objective function values throughout the two estimation case studies

Experimental case	Objective function value using		Improvement
	reference parameters	estimated parameters	
C1	0.498	0.356	28.5 %
C2	461.289	80.950	82.5 %

535

536 **Table II.** Parameter sets defined for the two estimation case scenarios and the generally applicable case, considering the minimum and
 537 maximum values taken by the SA method and the calculated average values ^a

Parameter category	Parameter	Initial value	Values taken in C1			Values taken in C2			General case (C*)		
			Min	Max	Avg	Min	Max	Avg	Min	Max	Avg
Hydrolysis yield coefficients	Hydr _{carb,in}	0.500	0.128	0.328	0.213	0.303	0.432	0.382	0.128	0.432	0.298
	Hydr _{prot,in}	0.200	0.202	0.295	0.256	0.152	0.309	0.228	0.152	0.309	0.242
Half-saturation constants [g L ⁻¹]	K _{SAA}	3.500	1.988	2.968	2.481	0.711	3.373	2.175	0.711	3.373	2.328
	K _{SHPr}	0.259	0.035	0.179	0.113	0.074	0.204	0.137	0.035	0.204	0.125
	K _{SHVal}	0.176	0.015	0.111	0.068	0.110	0.193	0.143	0.015	0.193	0.106
	K _{SHAc}	0.120	0.419	0.599	0.527	0.437	0.604	0.546	0.419	0.604	0.537
Inhibition constant [g L ⁻¹]	K _{iNH₃,HAc}	0.259	0.224	0.310	0.264	0.233	0.330	0.285	0.224	0.330	0.275
Higher pH	pK _{hAc}	8.5	8.345	9.643	8.893	8.450	9.248	8.759	8.345	9.643	8.826

boundary

Cell death rates [d ⁻¹]	Kd _{AA}	0.050	0.089	0.117	0.103	0.025	0.154	0.095	0.025	0.154	0.099
	Kd _{HPr}	0.050	0.109	0.134	0.119	0.114	0.174	0.144	0.109	0.174	0.132
	Kd _{HBut}	0.050	0.040	0.069	0.053	0.019	0.111	0.076	0.019	0.111	0.065
	Kd _{HVal}	0.050	0.027	0.115	0.067	0.057	0.170	0.100	0.027	0.170	0.084
	Kd _{HAc}	0.050	0.026	0.050	0.041	0.010	0.018	0.013	0.010	0.050	0.027

538

539 ^a Where *Hydr* are the hydrolysis constants; *carb,in* and *prot,in* indicate inert carbohydrate and protein substrates; *K_{s,sub}* are the half-
540 saturation constants of substrates; *AA* indicates soluble proteins; *HPr*, *HBut*, *HVal* and *HAc* are propionic, butyric, valeric and acetic acid,
541 respectively; *K_{iNH3.HAc}* is the ammonia inhibition constant effective on methanogenic microorganisms; *pK_{hAc}* is the upper pH limit where
542 the microorganic growth rates are approximately 50% of the uninhibited rate; *K_{d,sub}* are the death rates of substrate degrading microorganic
543 cells. Default and suggested parameter values are shown in bold.

544 **Figure legends**

545 **Figure 1.** Flowsheet representation of the systematic methodology used for analysis.

546 **Figure 2.** C1 and C2: Comparison of experimental and simulated biogas productivity,
547 where *BM_ben* indicates the BioModel benchmark simulation and *BM_opt*
548 indicates the BioModel simulation after the parameter estimation with the
549 best objective function. *ADM1* indicates the ADM1 simulation carried out by
550 Schön. Dashed vertical lines represent the boundaries between feeding
551 periods.

552 **Figure 3.** PRCC values of the most sensitive parameters in the two calibration case
553 scenarios. Each indicator output variable is represented by a different
554 polygon, and the peaks indicate the effects of respective parameters on the
555 variable, on a scale of -1 to 1. Abbreviations are as in Table II.

556 **Figure 4.** V1: Comparison of experimental and simulated biogas productivity (top) and
557 total VFA concentrations (bottom), where *BM_ben* indicates the BioModel
558 benchmark simulation and *BM_opt* indicates the BioModel simulation with
559 optimized parameters. Dashed vertical lines represent the boundaries between
560 feeding periods.

561 **Figure 5.** V2: Comparison of experimental and simulated methane productivity (top),
562 total VFA concentrations (middle) and total ammonia concentrations
563 (bottom), where *BM_Fit* indicates the BioModel simulation with default
564 parameters (carried out by Fitamo et al.) and *BM_opt* indicates the BioModel
565 simulation with optimized parameters. Dashed vertical lines represent the
566 boundaries between feeding periods.

567 **Figure 6.** V3: Comparison of experimental and simulated biogas productivity (top) and
568 total VFA concentrations (bottom), where *BM_ben* indicates the BioModel
569 benchmark simulation, *BM_opt* indicates the BioModel simulation with
570 optimized parameters and *ADM1* indicates the ADM1 simulation carried out
571 by Fezzani & Cheikh. Dashed vertical lines represent the boundaries between
572 feeding periods.

573

Figures

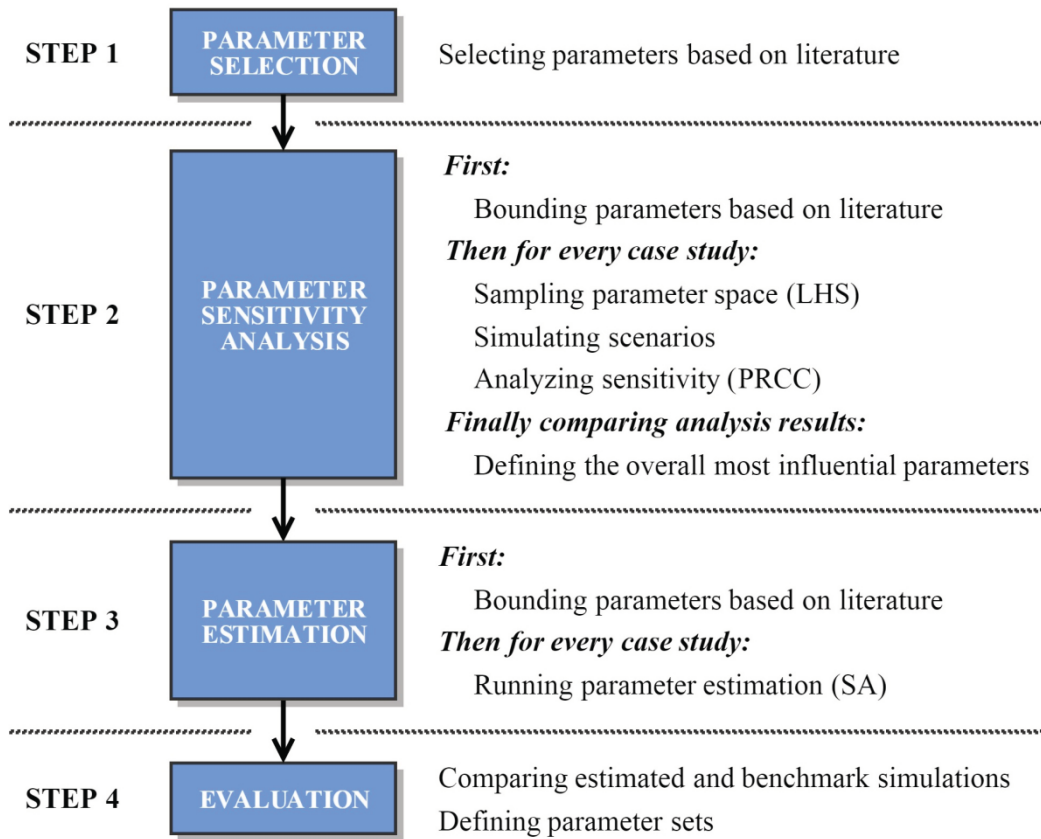
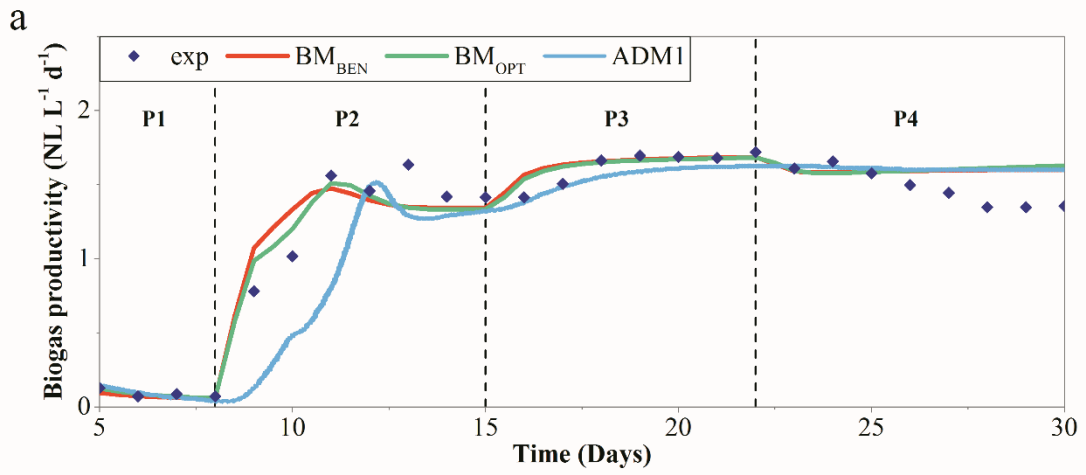
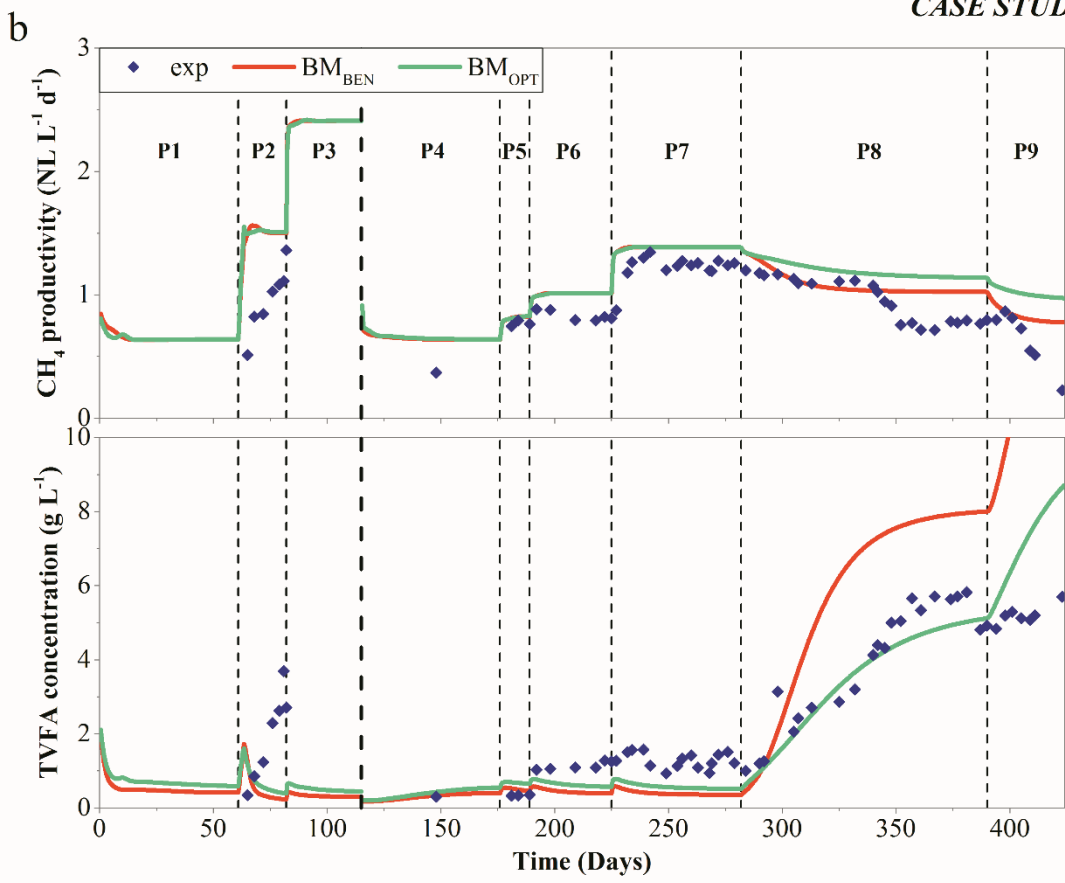


Figure 1



CASE STUDY 1

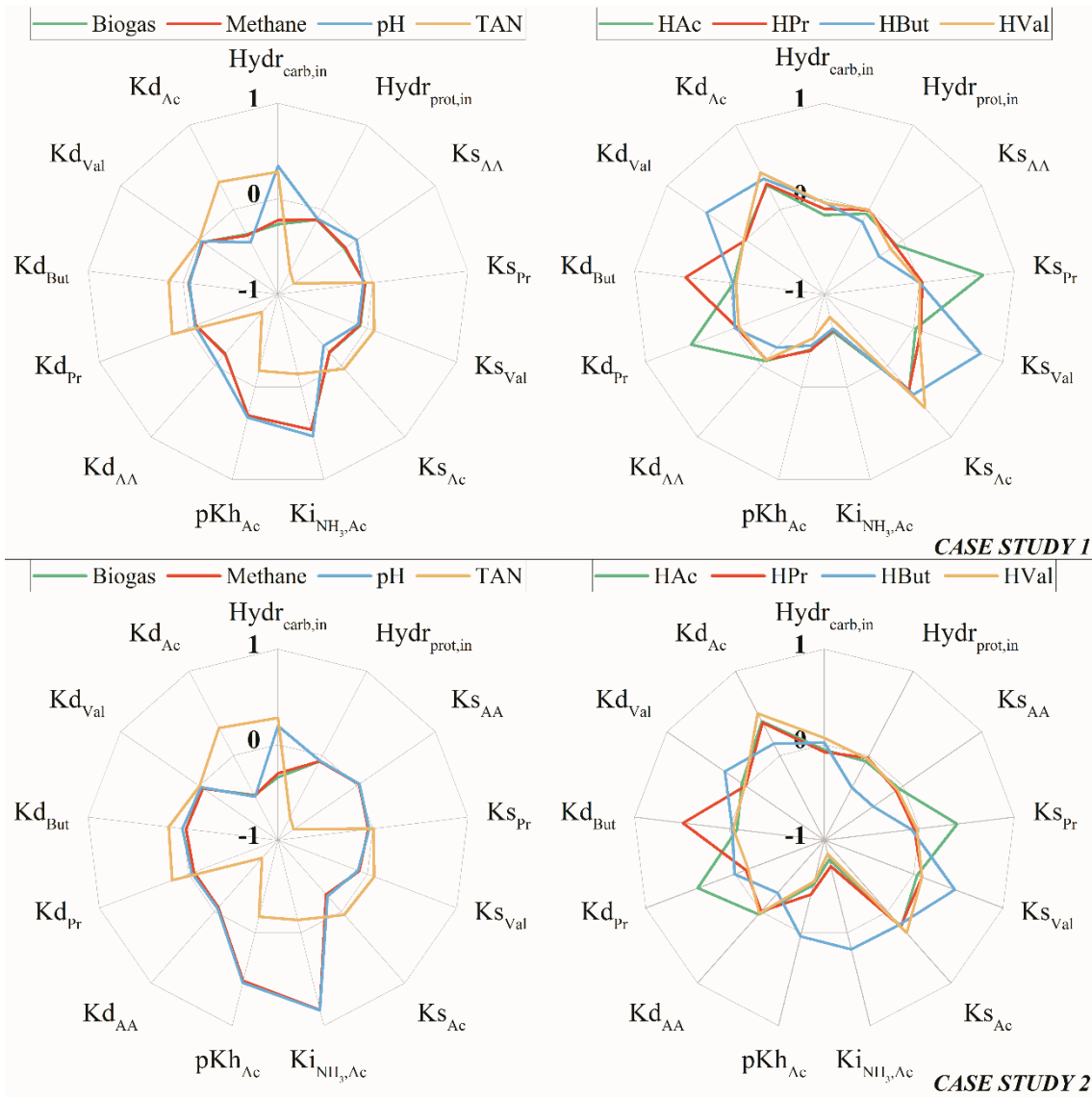


CASE STUDY 2

577

578

Figure 2

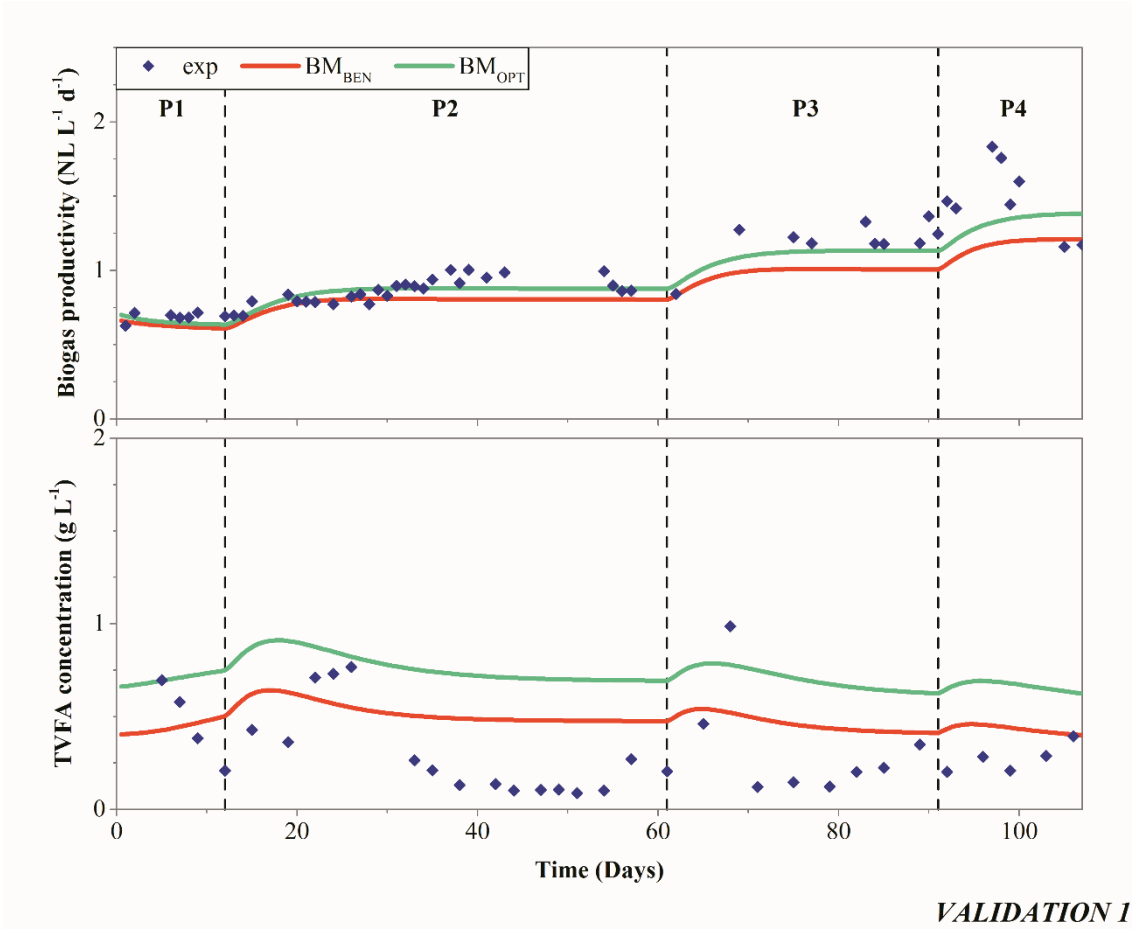


580

581

Figure 3

582

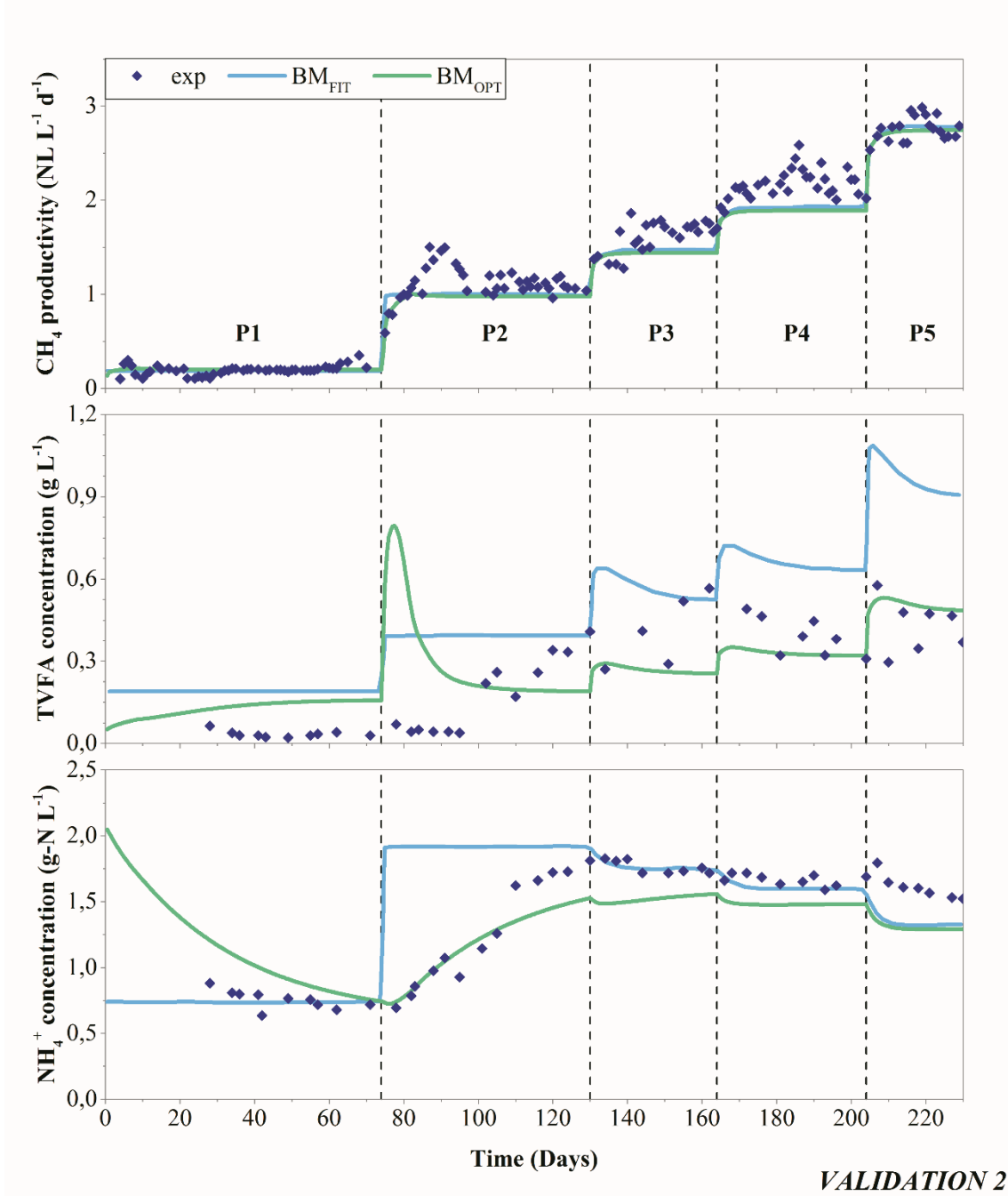


583

VALIDATION 1

584

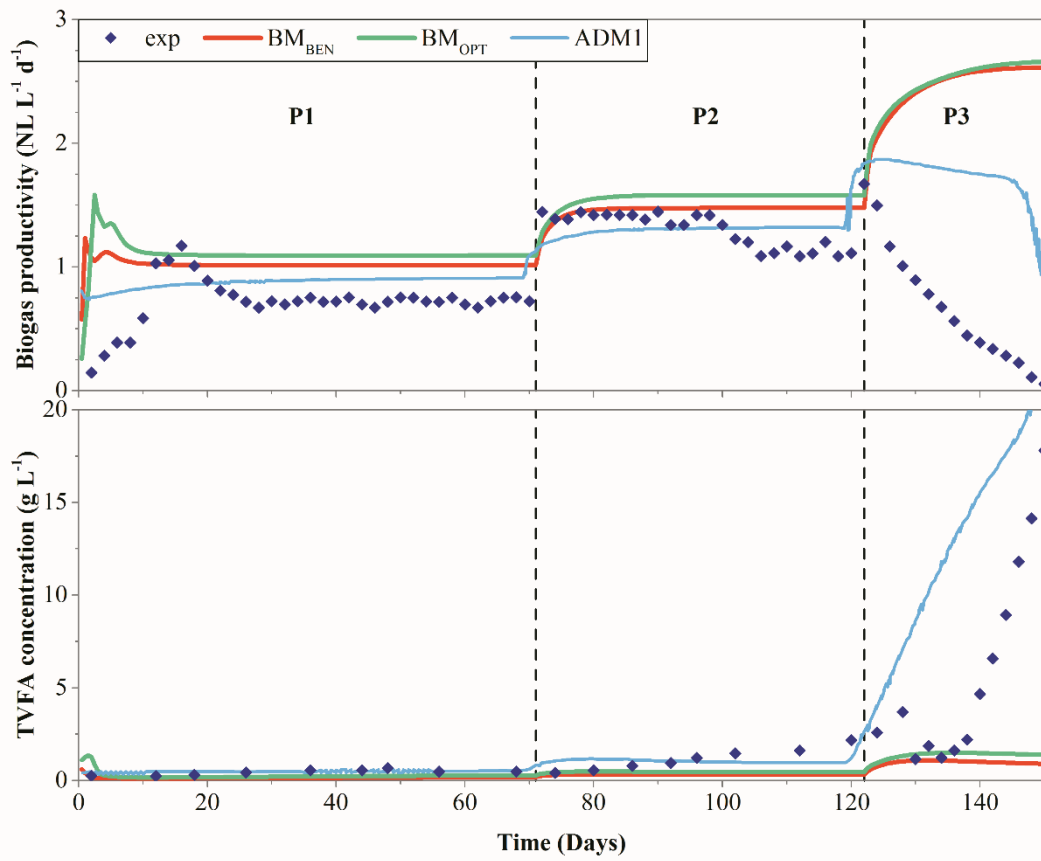
Figure 4



586

587

Figure 5



VALIDATION 3

588

589

Figure 6